



# Electrochemical advanced oxidation processes using novel electrode materials for mineralization and biodegradability enhancement of nanofiltration concentrate of landfill leachates

Marwa El Kateb <sup>a, b, d</sup>, Clément Trelu <sup>a, c, \*</sup>, Alaa Darwich <sup>a</sup>, Matthieu Rivallin <sup>a</sup>, Mikhael Bechelany <sup>a</sup>, Sakthivel Nagarajan <sup>a</sup>, Stella Lacour <sup>a</sup>, Nizar Bellakhal <sup>d</sup>, Geoffroy Lesage <sup>a</sup>, Marc Héran <sup>a</sup>, Marc Cretin <sup>a, \*</sup>

<sup>a</sup> IEM, Univ Montpellier, CNRS, ENSCM, Montpellier, France

<sup>b</sup> Université de Tunis El Manar, Faculté des Sciences de Tunis, 2092, Tunis, Tunisia

<sup>c</sup> Laboratoire Géomatériaux et Environnement, LGE – Université Paris-Est, EA 4508, UPEM, 77454, Marne-la-Vallée, France

<sup>d</sup> Université de Carthage, Institut National des Sciences Appliquées et de Technologie, Laboratoire d'Echo-Chimie, 1080, Tunis, Tunisia

## ARTICLE INFO

### Article history:

Received 27 April 2019

Received in revised form

1 July 2019

Accepted 3 July 2019

Available online 5 July 2019

### Keywords:

Electro-fenton

Anodic oxidation

Modified carbon felt

Sub-stoichiometric titanium oxide

Landfill leachate

Biodegradability

## ABSTRACT

The objective of this study was to implement electrochemical advanced oxidation processes (EAOPs) for mineralization and biodegradability enhancement of nanofiltration (NF) concentrate from landfill leachate initially pre-treated in a membrane bioreactor (MBR). Raw carbon felt (CF) or Fe<sup>II</sup>/Fe<sup>III</sup> layered double hydroxides-modified CF were used for comparing the efficiency of homogeneous and heterogeneous electro-Fenton (EF), respectively. The highest mineralization rate was obtained by heterogeneous EF: 96% removal of dissolved organic carbon (DOC) was achieved after 8 h of electrolysis at circumneutral initial pH (pH<sub>0</sub> = 7.9) and at 8.3 mA cm<sup>-2</sup>. However, the most efficient treatment strategy appeared to be heterogeneous EF at 4.2 mA cm<sup>-2</sup> combined with anodic oxidation using Ti<sub>4</sub>O<sub>7</sub> anode (energy consumption = 0.11 kWh g<sup>-1</sup> of DOC removed). Respirometric analyses under similar conditions than in the real MBR emphasized the possibility to recirculate the NF retentate towards the MBR after partial mineralization by EAOPs in order to remove the residual biodegradable by-products and improve the global cost effectiveness of the process. Further analyses were also performed in order to better understand the fate of organic and inorganic species during the treatment, including acute toxicity tests (Microtox<sup>®</sup>), characterization of dissolved organic matter by three-dimensional fluorescence spectroscopy, evolution of inorganic ions (ClO<sub>3</sub><sup>-</sup>, NH<sub>4</sub><sup>+</sup> and NO<sub>3</sub><sup>-</sup>) and identification/quantification of degradation by-products such as carboxylic acids. The obtained results emphasized the interdependence between the MBR process and EAOPs in a combined treatment strategy. Improving the retention in the MBR of colloidal proteins would improve the effectiveness of EAOPs because such compounds were identified as the most refractory. Enhanced nitrification would be also required in the MBR because of the release of NH<sub>4</sub><sup>+</sup> from mineralization of refractory organic nitrogen during EAOPs.

© 2019 Elsevier Ltd. All rights reserved.

## 1. Introduction

Rainwater percolation through waste layers of landfills generates leachates containing a complex mixture of dissolved organic matter (DOM), inorganic compounds, heavy metals, and xenobiotic

organic substances (Kjeldsen et al., 2002), which represents a significant hazard for the environment.

The implementation of a membrane bioreactor (MBR) followed by a nanofiltration (NF) step is one of the most efficient treatment strategy currently used for management of landfill leachates (Campagna et al., 2013; Amaral et al., 2016). However, NF is only a separation process. Biorefractory organic pollutants are accumulated and concentrated. Thus, the concentrate becomes an important residual issue for this treatment strategy (Van der Bruggen et al., 2003; Zhang et al., 2009, 2013). Landfill discharge of the

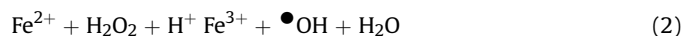
\* Corresponding authors. IEM, Univ Montpellier, CNRS, ENSCM, Montpellier, France.

E-mail addresses: [clement.trelu@u-pem.fr](mailto:clement.trelu@u-pem.fr) (C. Trelu), [marc.cretin@umontpellier.fr](mailto:marc.cretin@umontpellier.fr) (M. Cretin).

concentrate is commonly performed. However, some national regulations do not allow such practice and it clearly does not fix the long-term issue. In recent years, several processes have been investigated and applied at industrial scale for the treatment of NF concentrate. For example, adsorption processes are effective to remove organic matters in NF concentrate, but they are strongly limited by the high organic charge of such effluents compared to the adsorption capacity of adsorbent materials. Besides, membrane distillation and evaporation processes are substantially limited by the high cost of equipment and energy consumption (Cui et al., 2018).

During the last two decades, electrochemical advanced oxidation processes (EAOPs) have received great attention for efficient degradation of a large range of hazardous and biorefractory organic compounds. They are based on *in situ* electrogeneration of hydroxyl radicals ( $\bullet\text{OH}$ ), a non-selective and powerful oxidizing agent ( $E^\circ(\bullet\text{OH}/\text{H}_2\text{O}) = 2.80\text{ V vs SHE}$ ) (Brillas et al., 2009; Comninellis et al., 2008; Martínez-Huitle et al., 2015; Panizza and Cerisola, 2009). EAOPs provide also several technical advantages such as high versatility, easy operation, possibility for automation and low consumption of chemical reagents (Radjenovic and Sedlak, 2015; Sirés et al., 2014). However, complete mineralization of organic compounds requires high energy consumption. Therefore, the combination of EAOPs with biological processes is currently more and more investigated as a feasible option for improving the global cost-effectiveness of the process (Oller et al., 2011; Ganzenko et al., 2014, 2018; Trellu et al., 2016a; Olvera-Vargas et al., 2015). In order to achieve reliable conclusions, the accurate assessment of biodegradability enhancement by EAOPs requires the use of proper measurement tools such as respirometric methods (Reuschenbach et al., 2003).

Anodic oxidation (AO) and electro-Fenton (EF) are the most popularized EAOPs (Brillas et al., 2009; Panizza and Cerisola, 2009; Martínez-Huitle et al., 2015; Oturan et al., 2015). AO is based on the generation of hydroxyl radicals ( $\bullet\text{OH}$ ) via water oxidation at the surface of anodes (M) with high overvoltage for oxygen evolution reaction (Eq. (1)) (Panizza and Cerisola, 2009; Trellu et al., 2017; Özcan et al., 2008), while  $\bullet\text{OH}$  are generated homogeneously in the bulk during the EF process through the Fenton's reaction (Eq. (2)) (Brillas et al., 2009; Ma et al., 2016; Zhang et al., 2007).  $\text{H}_2\text{O}_2$  and iron (II) are continuously electrogenerated at the cathode by reduction of dissolved oxygen (Eq. (3)) and iron (III) reduction (Eq. (4)), respectively. External oxygen supply is required and an iron source must be either initially added at catalytic amount to the treated solution (homogeneous EF) or embedded onto suitable electrode materials (heterogeneous EF).



Homogeneous EF requires external iron source and acidic pH (*i.e.* pH 2.5–3.5) that prevents iron precipitation (Brillas et al., 2009). Besides, heterogeneous EF using for example pyrite (Ammar et al., 2015) or iron loaded sepiolite (Iglesias et al., 2013) as iron source has been developed in order to operate the process over a wide pH range (Ganiyu et al., 2018a, b; Poza-Nogueiras et al., 2018). Innovative electrodes have been also synthesized and studied as both heterogeneous catalyst source and cathode materials (Zhang et al., 2012; Wang et al., 2013; García-Rodríguez et al., 2016; Ganiyu et al., 2017a). Particularly, the modification of raw carbon

felt (CF) with CoFe or  $\text{Fe}^{\text{II}}\text{Fe}^{\text{III}}$ -layered double hydroxide (LDH) also led to an increase of the electroactive surface area, which in turn improved the generation of  $\text{H}_2\text{O}_2$  and the global efficiency of the heterogeneous EF process (Ganiyu et al., 2017a, 2018a, b). However, to the best of our knowledge, none study focused on the application of such promising electrodes for the treatment of real wastewaters.

As regards to anode materials, sub-stoichiometric titanium oxides (especially  $\text{Ti}_4\text{O}_7$ ) recently received great attention for application in wastewater treatment by AO (Guo et al., 2016; Ganiyu et al., 2016; Trellu et al., 2018b).  $\text{Ti}_4\text{O}_7$  anode is able to generate large amounts of physisorbed hydroxyl radicals ( $\text{Ti}_4\text{O}_7(\bullet\text{OH})$ ) for the degradation and mineralization of organic contaminants. Besides, this material has the potential to become a low-cost anode compared to the well known boron-doped diamond anode (Ganiyu et al., 2017b; Trellu et al., 2018b). However, to the best of our knowledge, such anode material has also still not been applied for the treatment of real effluents.

The objective of this study was to investigate the application of these novel electrode materials for the treatment of a NF concentrate of landfill leachate initially pre-treated in a MBR, which represents an important challenge for environmental engineering. Various configurations (*i.e.* homogeneous EF, heterogeneous EF, heterogeneous EF/AO) and operating conditions were studied. The efficiency for mineralization of organic compounds was compared. A particular attention was also given to the understanding of mineralization mechanisms by using various analytical tools: (i) DOM was characterized by three-dimensional excitation and emission matrix fluorescence (3DEEM), (ii) degradation by-products such as short-chain carboxylic acids were identified and quantified by ion-exclusion HPLC, and (iii) inorganic ions released during the mineralization process were identified and quantified by ion chromatography. Moreover, acute toxicity of the effluent was assessed by Microtox<sup>®</sup> analysis and the possibility to use such EAOPs as a pre-treatment before recirculation towards the MBR was assessed by using respirometric method under similar conditions than in the real industrial MBR. Finally, recommendations were given by taking into consideration the interdependence of MBR process and EAOP in a combined treatment strategy.

## 2. Materials and methods

### 2.1. Chemicals

For the preparation of  $\text{Fe}^{\text{II}}\text{Fe}^{\text{III}}$ -LDH modified CF, iron III nitrate nonahydrate  $\text{Fe}(\text{NO}_3)_3 \cdot 9\text{H}_2\text{O}$  (CAS 7782-61-8, 98% purity), iron II sulfate heptahydrate  $\text{FeSO}_4 \cdot 7\text{H}_2\text{O}$  (CAS 7782-63-0, >99% purity), urea  $\text{CO}(\text{NH}_2)_2$  (CAS 57-13-6) and ammonium fluoride  $\text{NH}_4\text{F}$  (CAS 12,125-01-8, 99% purity) were supplied by Sigma Aldrich. Ultra-pure water (Millipore Mill-Q system, resistivity >18  $\text{M}\Omega\text{ cm}$  at 25 °C) was used for the preparation of all solutions.

### 2.2. Landfill leachate (NF concentrate)

The NF concentrate was collected from a landfill leachate wastewater treatment plant (WWTP) in the south of France. The raw landfill leachate was initially treated in a MBR, then followed by a NF step. The concentrate from the NF step was collected and stored in a refrigerator at 4 °C.

### 2.3. Electrochemical setup and electrode materials

Experiments were conducted in an undivided cylindrical glass containing 220 mL of NF concentrate at room temperature (25 °C). The electrochemical cell was similar to the one used in several previous studies (Ganiyu et al., 2016; Trellu et al., 2016b). Either raw

CF (for homogeneous EF) or Fe<sup>II</sup>Fe<sup>III</sup>-LDH modified CF (for heterogeneous EF) was employed as cathode (20 × 6 cm; 120 cm<sup>2</sup>), positioned on the inner wall of the cylindrical cell. CF (99.0%, 6.35 mm thick) was provided by Alfa Aesar. Fe<sup>II</sup>Fe<sup>III</sup>-LDH modified CF was prepared by *in-situ* solvothermal process as reported elsewhere (Ganiyu et al., 2018a, b). LDH coating was 0.62 ± 0.04 mg cm<sup>-2</sup>, which was also in agreement with what has been reported previously (Ganiyu et al., 2018a, b). For homogeneous EF experiments, 0.2 mM of Fe<sup>2+</sup> was added to the solution and initial pH was adjusted at 3 (values usually reported as optimal). For heterogeneous EF experiments, none Fe<sup>2+</sup> was externally added and pH was not initially adjusted.

The anode was either a 24 cm<sup>2</sup> (3 × 8 cm) platinum mesh (for homogeneous and heterogeneous EF) or a 32 cm<sup>2</sup> (4 × 8 cm) Ti<sub>4</sub>O<sub>7</sub> thin film plasma deposited on Ti substrate (for heterogeneous EF/AO) from Saint-Gobain Research Provence, France. Ti<sub>4</sub>O<sub>7</sub> powder used for plasma deposition was prepared by carbothermal reduction of TiO<sub>2</sub> as already reported by our group (Ganiyu et al., 2016, 2017b). These rectangular-shaped anodes were placed at the center of the cylindrical electrochemical cell, with an average interelectrode distance of 3 cm.

Electrodes were connected to a DC power supply (CNB Electronique) with applied current set at 1000 mA ( $j = 8.3 \text{ mA cm}^{-2}$ , calculated from the cathode surface, which is the working electrode during the EF process) or 500 mA ( $j = 4.2 \text{ mA cm}^{-2}$ ). A magnetic stirrer was used to improve mass transport of chemical species toward/from the electrodes. The solution was saturated with O<sub>2</sub> by bubbling compressed air through a glass frit 10 min before starting the experiments and all along the electrolysis. The conductivity of the NF concentrate was high enough to ensure the electrolysis without any additional supporting electrolyte. For comparison, a reference experiment was also carried out using raw carbon felt cathode, Pt anode, without adding any source of iron and without initial pH adjustment.

#### 2.4. Dissolved organic carbon and chemical oxygen demand analysis

Mineralization rate of NF concentrate was determined by total organic carbon (TOC) analyses using the Shimadzu TOC-L analyzer based on the 680 °C combustion catalytic oxidation method. All samples were filtrated through 0.45 μm regenerated cellulose (RC) membrane filters. Therefore, results are reported as dissolved organic carbon (DOC).

Chemical oxygen demand (COD) was analyzed by the method AFNOR NFT 90–101 using Hach COD kits.

#### 2.5. Respirometric method for the determination of biodegradability

Biodegradability was assessed with a BM-T Advance Respirometer (SURCIS S.L, Spain), which consists in a 1 L capacity vessel, provided with an oxygen probe (Hamilton) and temperature control system. The activated sludge used in the bioassays was collected from the aerated tank of the landfill leachate WWTP using MBR and was thus acclimatized to the effluent. The samples were evaluated without pH adjustment because of the high buffer capacity of the landfill leachate samples. Continuous aeration and agitation were applied to ensure air saturation conditions. Temperature was maintained at 20 °C during the tests and the standardization with sodium acetate method was applied (conversion rate adjustment according to instructions given by the respirometer's manufacturer). In order to inhibit the nitrification process and measure the sample effect only on the heterotrophic bacteria, 1.5 mg gVSS<sup>-1</sup> of N-allylthiourea was added before the beginning of

each trial.

For biodegradability assays, 700 mL of endogenous activated sludge and 300 mL of target sample were introduced in the respirometer. The biodegradability of samples pre-treated by EAOPs was assessed through R tests (Fig. SI 1). The ratio between biodegradable COD (bCOD) and DOC (bCOD/DOC) was used for determination of the biodegradable character of each sample. A biodegradability enhancement index (BE) was calculated by using Eq. (5).

$$BE = \frac{\left(\frac{bCOD_t}{DOC_t}\right)}{\left(\frac{bCOD_0}{DOC_0}\right)} \quad (5)$$

Where bCOD<sub>t</sub> and DOC<sub>t</sub> are bCOD (in gO<sub>2</sub> L<sup>-1</sup>) and DOC (in gC L<sup>-1</sup>) after t hours of treatment by EAOPs.

#### 2.6. Characterization of dissolved organic matter by three-dimensional excitation and emission matrix fluorescence (3DEEM)

Natural organic matter was characterized by 3DEEM fluorescence using a PerkinElmer LS-55 spectrometer (USA). The dilution factor was 200 for all samples. The procedure reported by Jacquin et al. (2017) was used for fluorescence spectra acquisition and data extraction. Chen et al. (2003) divided fluorescence spectra into five different areas corresponding to different groups of fluorophores, *i.e.* regions I and II for aromatic proteins, region III for fulvic acid-like (FA-like) fluorophores, region IV for soluble microbial by-product-like (SMP-like) fluorophores and region V for humic acid-like (HA-like) fluorophores (Chen et al., 2003). Similarly to the study of Jacquin et al. (2017), 3DEEM results were analyzed by taking into consideration only 3 different zones, *i.e.* zone I' for region I + II (aromatic proteins), zone II' for region IV (SMP-like) and zone III' for region III + V (HA + FA-like). Calculation of the volume of fluorescence in these different zones was achieved following the method from Jacquin et al. (2017).

The procedures for ICP-MS analysis, toxicity test (Microtox<sup>®</sup>), identification/quantification of inorganic ions and identification/quantification of short-chain carboxylic acids are provided in Supplementary Information (SI).

### 3. Results and discussion

#### 3.1. Characterization of the NF concentrate effluent

The characteristics of the NF concentrate are presented in SI (Table SI 1). The effluent was a dark brown liquid having a slightly alkaline pH and high organic charge. The conductivity (3.1 mS cm<sup>-1</sup>) was between 3 and 10 times lower than values reported in the literature (10–33 mS cm<sup>-1</sup>) (Li et al., 2015; Hu et al., 2018; Xu et al., 2017). This might be ascribed to the high diversity of landfill leachate and to a lower retention of ionic species by the NF step. In fact, the concentration factor of divalent (Mg<sup>2+</sup> and Ca<sup>2+</sup>) and monovalent (Na<sup>+</sup> and K<sup>+</sup>) inorganic cations was only 3.1 ± 0.3 and 1.7 ± 0.2, respectively. Monovalent ions are less retained by the NF membrane because of lower charge interactions (Van der Bruggen et al., 2004). The COD content (2.1 gO<sub>2</sub> L<sup>-1</sup>) of the NF concentrate was also in the low range of values usually reported in the literature (1.7–5.5 gO<sub>2</sub> L<sup>-1</sup>) (Li et al., 2015; Hu et al., 2018; Xu et al., 2017) because of (i) operation of the NF process with a lower concentration factor and/or (ii) lower initial organic loading rate of the effluent pre-treated by the MBR.

The ratio between bCOD and total COD or total DOC was low (bCOD/COD = 0.12 or bCOD/DOC = 0.26), thus indicating the low biodegradability of the concentrate owing to the presence of high-

molecular weight and non-biodegradable compounds. A high concentration of nitrate ( $[\text{NO}_3^-] = 90 \text{ mg L}^{-1}$ ) was observed due to the complete nitrification of  $\text{NH}_4^+$  in the MBR and a partial denitrification in the anoxic tank. As regards to metals, Sr ion was the most concentrated ( $6.0 \text{ mg L}^{-1}$ ) and high concentrations of As ( $0.38 \text{ mg L}^{-1}$ ) and Cr ( $0.67 \text{ mg L}^{-1}$ ) ions were also reported. These metals are released by different wastes discarded in landfills such as glass products (Ponthieu et al., 2007), fluorescent lights and ceramics (Mahindrakar and Rathod, 2018). Besides, the high concentration of Sb ( $1.2 \text{ mg L}^{-1}$ ) indicates an important contamination from plastic decomposition (Westerhoff et al., 2008).

### 3.2. Mineralization efficiency by EAOPs

Various experiments were performed in order to evaluate the efficiency of different EAOPs (i.e. homogeneous EF, heterogeneous EF, heterogeneous EF/AO).

First, volatilization and adsorption phenomena were evidenced by bubbling oxygen into the electrochemical reactor without any current applied. Under these conditions, DOC content decreased and reached a plateau after 1 h with around  $16 \pm 2\%$  removal due to volatilization of volatile organic compounds and adsorption of hydrophobic compounds on CF. Besides, it was also observed that initial pH adjustment at 3 decreased the DOC value by  $15 \pm 5\%$  because of the precipitation of humic acids.

Second, experiments were carried out under constant current density applied to the electrodes. As shown in Fig. 1A, 96% of DOC removal was obtained after 8 h of electrolysis by heterogeneous EF with an applied current density of  $8.3 \text{ mA cm}^{-2}$ . The excellent mineralization efficiency achieved without any initial pH adjustment was ascribed to heterogeneous EF reaction occurring on the surface of the  $\text{Fe}^{\text{II}}\text{Fe}^{\text{III}}$ -LDH catalyst, which catalyzed the decomposition of  $\text{H}_2\text{O}_2$  to generate large amounts of hydroxyl radicals  $\bullet\text{OH}$  (Ganiyu et al., 2018a, b). By comparison, only 59% removal of DOC was obtained in the reference experiment with analogous operating conditions but using raw CF as cathode instead of  $\text{Fe}^{\text{II}}\text{Fe}^{\text{III}}$ -LDH modified CF, thus highlighting the benefits obtained from the use of the modified cathode. Heterogeneous EF was also even more efficient than conventional homogeneous EF (90% removal of DOC after 8 h) with external addition of iron catalyst ( $0.2 \text{ mmol L}^{-1}$ ) and initial adjustment of pH at 3. Therefore,  $\text{Fe}^{\text{II}}\text{Fe}^{\text{III}}$ -LDH modified CF

appeared as an ideal cathode material that enhances the mineralization efficiency of the EF process and avoids both initial pH adjustment and external addition of iron. The stability and reusability of the prepared  $\text{Fe}^{\text{II}}\text{Fe}^{\text{III}}$ -LDH modified CF cathode was assessed by reusing the same electrode for 4 successive electrolysis cycles (Fig. 2). The slight but continuous decrease of the efficiency could be ascribed to (i) the initial loss of loosely bounded  $\text{Fe}^{\text{II}}\text{Fe}^{\text{III}}$ -LDH at the external surface of the CF substrate due to vigorous stirring and/or (ii) iron leaching at acidic pH for which  $\text{Fe}^{\text{II}}\text{Fe}^{\text{III}}$ -LDH coating is less stable. Indeed, a progressive reduction of pH to values in the range 3–4 was noticed during electrolysis, which was explained by the generation of short-chain carboxylic acids. This leaching phenomenon was confirmed by comparison of SEM images of raw CF,  $\text{Fe}^{\text{II}}\text{Fe}^{\text{III}}$ -LDH modified CF before use and  $\text{Fe}^{\text{II}}\text{Fe}^{\text{III}}$ -LDH modified CF after 4 cycles of electrolysis (Fig. SI 2). While an extensive growth on the CF of dense platelets of  $\text{Fe}^{\text{II}}\text{Fe}^{\text{III}}$ -LDH with uneven and porous structure was initially obtained, a partial degradation of the global  $\text{Fe}^{\text{II}}\text{Fe}^{\text{III}}$ -LDH structure was observed after 4 cycles. Thus, in order to avoid the depletion of the catalyst, a continuous pH control regulation would be recommended rather

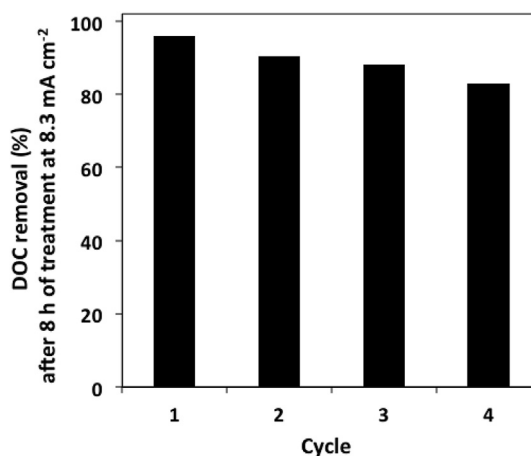


Fig. 2. DOC removal after 8 h of electrolysis vs number of cycles for the heterogeneous EF treatment using  $\text{Fe}^{\text{II}}\text{Fe}^{\text{III}}$ -LDH/CF cathode and Pt anode at  $8.3 \text{ mA cm}^{-2}$ .

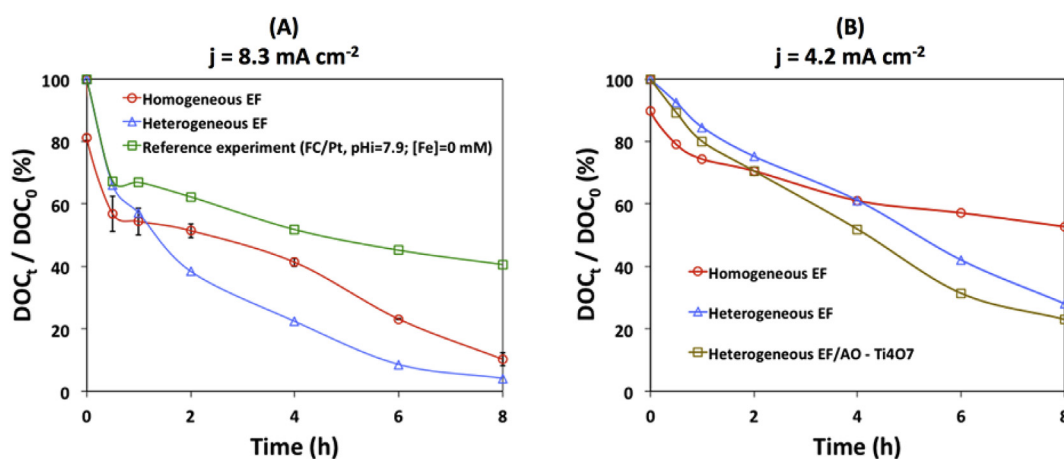


Fig. 1. DOC removal efficiency vs time during the mineralization of NF concentrate. Comparison of different configurations and operating conditions. (A)  $J = 8.3 \text{ mA cm}^{-2}$ : (○) Homogeneous EF with CF cathode, Pt anode,  $[\text{Fe}^{2+}] = 0.2 \text{ mmol L}^{-1}$ ,  $\text{pH}_0 = 3$ ; (△) Heterogeneous EF with  $\text{Fe}^{\text{II}}\text{Fe}^{\text{III}}$ -LDH modified CF cathode, Pt anode,  $[\text{Fe}^{2+}] = 0 \text{ mmol L}^{-1}$ ,  $\text{pH}_0 = 7.9$ ; (□) Reference experiment with CF cathode, Pt anode,  $[\text{Fe}^{2+}] = 0 \text{ mmol L}^{-1}$ ,  $\text{pH}_0 = 7.9$ . Three homogeneous EF experiments were performed in order to assess the reproducibility of the experimental procedure. Standard deviations are reported in Fig. 1A. (B)  $J = 4.2 \text{ mA cm}^{-2}$ : (○) Homogeneous EF with CF cathode, Pt anode,  $[\text{Fe}^{2+}] = 0.2 \text{ mmol L}^{-1}$ ,  $\text{pH}_0 = 3$ ; (△) Heterogeneous EF with  $\text{Fe}^{\text{II}}\text{Fe}^{\text{III}}$ -LDH modified CF cathode, Pt anode,  $[\text{Fe}^{2+}] = 0 \text{ mmol L}^{-1}$ ,  $\text{pH}_0 = 7.9$ ; (□) Heterogeneous EF/AO with  $\text{Fe}^{\text{II}}\text{Fe}^{\text{III}}$ -LDH modified CF cathode,  $\text{Ti}_4\text{O}_7$  anode,  $[\text{Fe}^{2+}] = 0 \text{ mmol L}^{-1}$ ,  $\text{pH}_0 = 7.9$ .

than a unique pH re-adjustment at the end of the treatment.

Third, experiments were also performed at lower current density ( $4.2 \text{ mA cm}^{-2}$ , Fig. 1B). Lower DOC removal rates were obtained, e.g. 72% vs 96% removal of DOC after 8 h of treatment by heterogeneous EF at  $4.2 \text{ mA cm}^{-2}$  and  $8.3 \text{ mA cm}^{-2}$ , respectively. Indeed, high current density enhances the generation of hydrogen peroxide and regeneration rate of Fe(II). Thus, further  $\bullet\text{OH}$  are produced for oxidation and mineralization of organic compounds.

Fourth, the influence of the anode material was also investigated (Fig. 1B). After 8 h of treatment by heterogeneous EF/AO using  $\text{Ti}_4\text{O}_7$  anode at  $4.2 \text{ mA cm}^{-2}$ , 77% removal of DOC was achieved, compared to 72% by heterogeneous EF using Pt anode. The higher efficiency of  $\text{Ti}_4\text{O}_7$  anode was ascribed to the generation at the anode surface of physisorbed  $\text{Ti}_4\text{O}_7(\bullet\text{OH})$  with great oxidation ability, because of the higher overvoltage for oxygen evolution reaction ( $>0.7 \text{ V}$ ), compared to Pt anode ( $<0.4 \text{ V}$ ) (Trellu et al., 2018a; Ganiyu et al., 2018a, b). Therefore, by taking also into consideration the lower cost of  $\text{Ti}_4\text{O}_7$ , this anode material appeared as a suitable electrode to combine AO and EF processes.

One of the main challenges for EAOPs is to reduce the energy consumption (EC). The EC was expressed as kWh per g of DOC removed and calculated from Eq. (6) (Brillas et al., 2009).

$$EC_{\text{DOC}} \left( \text{kWh g}^{-1} \text{ of DOC} \right) = \frac{E_{\text{cell}} I t}{V \Delta(\text{DOC})_{\text{exp}}} \quad (6)$$

where  $E_{\text{cell}}$  is the average cell voltage (V),  $I$  the applied current (A),  $t$  the duration of electrolysis (h),  $V$  the volume of solution treated (L) and  $\Delta(\text{DOC})_{\text{exp}}$  the experimental decays of DOC ( $\text{mgC L}^{-1}$ ).

For example, 96% removal of DOC by heterogeneous EF at  $8.3 \text{ mA cm}^{-2}$  required  $0.35 \text{ kWh g}^{-1}$  of DOC removed. By comparison, 77% DOC removal by heterogeneous EF/AO using  $\text{Ti}_4\text{O}_7$  anode at  $4.2 \text{ mA cm}^{-2}$  required only  $0.13 \text{ kWh g}^{-1}$  of DOC. This value decreased to  $0.11 \text{ kWh g}^{-1}$  of DOC for 45% removal of DOC by the same process (4 h of treatment instead of 8 h). In fact, high current density strongly increased energy consumption because of concomitant rise in total cell voltage (from 7.2 to 10.4 V). Parasitic reaction such as hydrogen evolution,  $4 \text{ e}^-$  reduction of  $\text{O}_2$  to  $\text{H}_2\text{O}$  and  $2 \text{ e}^-$  oxidation of water to  $\text{O}_2$  are also promoted at higher current density. Moreover, at high removal rate of DOC and low residual DOC, the current efficiency is strongly decreased by mass transport limitations. Therefore, in order to achieve high DOC removal rate with low energy consumption, it was proposed to combine EAOPs with a biological post-treatment, since EAOPs are able to transform biorefractory organic compounds into by-products that are more biodegradable than initial compounds (Ganzenko et al., 2014; Olvera-Vargas et al., 2015; Trellu et al., 2016a). In practice, that would mean implementing the EAOP as a preliminary treatment before recirculation of the NF concentrate towards the MBR. Thus, the next objective of this study was to monitor the evolution of the biodegradability of the effluent, as well as to better understand the evolution of organic and inorganic compounds during EAOPs.

### 3.3. Biodegradability enhancement

Respirometric measurements performed have the advantage of being a direct and rapid biological assessment of aerobic degradation under similar conditions than in the real industrial MBR (Reuschenbach et al., 2003). The calculated biodegradability enhancement (BE) values are presented in Fig. 3 after 4 and 8 h of treatment for different EAOP configurations and current densities applied.

In all cases, heterogeneous EF shows an increase in the biodegradability of the NF concentrate, which validate the potential positive role of EAOPs as a pre-treatment before recirculating the

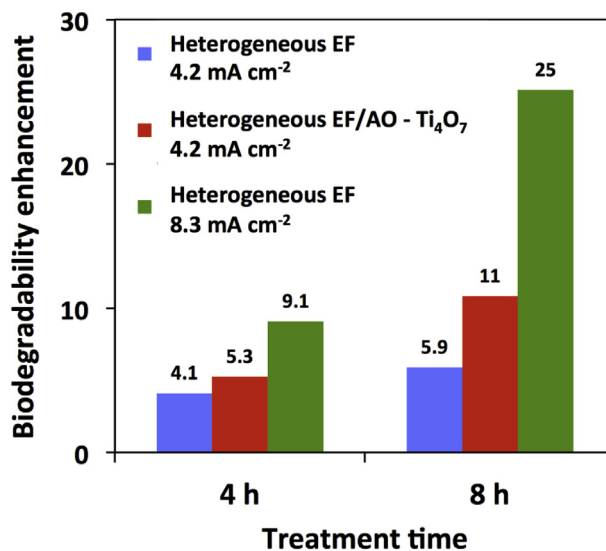


Fig. 3. Biodegradability enhancement at two different treatment times for different EAOPs and current densities.

NF concentrate to the MBR. In general the more the mineralization rate is achieved the more the biodegradability enhancement is observed. After 8 h of treatment by heterogeneous EF at  $4.2 \text{ mA cm}^{-2}$ , the BE index reached 11 with  $\text{Ti}_4\text{O}_7$  anode, compared to 5.9 with Pt anode, which validate the positive effect of combining EF with AO. We could state that a satisfactory biodegradability enhancement (between 4.1 and 9.1) was reached after 4 h with optimal energy consumption efficiency.

### 3.4. Acute toxicity of the effluent

Toxicity evolution of the NF concentrate during its electrolysis by both heterogeneous and homogeneous EF was evaluated by Microtox<sup>®</sup> standard method (Fig. 4). Initially (i.e. before any treatment of the NF concentrate), around  $50 \pm 5\%$  of *V. fischeri* luminescence inhibition was observed because of the presence of large amount of

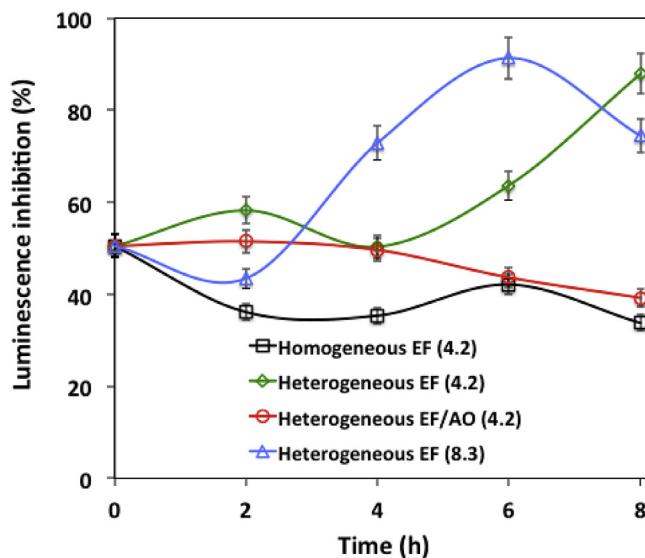


Fig. 4. Evolution of *Vibrio fischeri* luminescence inhibition (Microtox<sup>®</sup> test) vs electrolysis time according to EAOP configuration and current density (in brackets,  $\text{mA cm}^{-2}$ ).

toxic trace metals and organic pollutants. *V. fischeri* luminescence inhibition can be sensitive to various phenomena that can not be controlled and studied separately during the treatment of such complex effluent, e.g. the removal of toxic organic pollutants, the formation of toxic degradation by-products, the formation of non-toxic degradation by-products (which could promote stimulation of bacterial luminescence), the release of inorganic compounds and the evolution of metal speciation. Therefore, it is difficult to draw reliable conclusions from these analyses. However, results show that EAOPs are not able to remove completely the acute toxicity from such complex effluent containing both organic and inorganic toxic compounds. Luminescence inhibition might even increase significantly, particularly after achieving high mineralization rates (for example during heterogeneous EF at  $8.3 \text{ mA cm}^{-2}$  and heterogeneous EF at  $4.2 \text{ mA cm}^{-2}$ ). From the comparison of heterogeneous EF experiments performed with either Pt or  $\text{Ti}_4\text{O}_7$  anode, it seems that anodic oxidation participate to avoid the accumulation of toxic by-products in the bulk.

### 3.5. Characterization of the organic matter by 3DEEM

3DEEM has been reported to be a useful tool for characterization of colloidal and dissolved organic matter. Particularly, [Jacquin et al. \(2017\)](#) recently emphasized a correlation between the volume of fluorescence of zone III' (HA + FA-like fluorophores) and the concentration in a full-scale MBR of humic substances (MW  $\approx 1000$  Da) and building blocks (degradation by-products from humic substances, with MW  $\approx 300$ – $500$  Da) measured by size exclusion liquid chromatography coupled with organic carbon and organic nitrogen detector. Similarly, a correlation was also obtained between the volume of fluorescence of zone II' (SMP-like fluorophores) and the concentration of proteins from biopolymers (MW  $\approx 20,000$ – $7.5 \times 10^{11}$  Da). Besides, no correlation was obtained for the volume of fluorescence of zone I' because fluorophores of this zone would be mostly associated with colloidal proteins that could not be analyzed by size exclusion liquid chromatography ([Jacquin et al., 2017](#)). In this study, we proposed to use these results with the view to obtain indications on the evolution of the nature of the organic matter during EAOPs.

The initial effluent was mainly constituted of HA + FA-like fluorophores from zone III' as shown in [Fig. 5A](#) and [B](#). This result is consistent with the pre-treatment of the effluent in the MBR because microfiltration membranes have lower retention capacity for these low MW compounds. A strong decrease of fluorophores of zone III' was then observed during both heterogeneous EF ([Fig. 5C](#)) and EF/AO ([Fig. 5D](#)) due to (i) precipitation of humic acids at acidic pH and (ii) fast degradation and mineralization of these low MW compounds with an aromatic structure that reacts quickly with  $\bullet\text{OH}$  ([Trellu et al., 2016b](#)). By comparison, fluorescence from colloidal proteins of zone I' decreased much more slowly. This phenomenon might be ascribed to the lower availability of colloids for reaction with  $\bullet\text{OH}$  in the aqueous phase. In the context of the global combined process, this result means that improving the retention of colloidal proteins in the MBR would then have a positive effect on the efficiency of the EAOP. Finally, it was also observed that the use of  $\text{Ti}_4\text{O}_7$  anode for the heterogeneous AO/EF process promoted significantly the decrease of the fluorescence of proteins from biopolymers (zone II', [Fig. 5D](#)). This might be ascribed to the higher electro-catalytic activity of  $\text{Ti}_4\text{O}_7$  for anodic oxidation of organic compounds, compared to Pt anode ([Ganiyu et al., 2016](#)).

### 3.6. Identification and quantification of short-chain carboxylic acids

Short-chain carboxylic acids are common degradation by-products generated during the degradation of organic compounds

by EAOPs ([Oturán et al., 2008](#)). In this study, they were identified by ion-exclusion HPLC and chromatograms revealed five well defined peaks corresponding to acetic, formic, succinic, malonic and oxamic acids. Results were firstly analyzed by following the evolution of the concentration of the sum of carboxylic acids analyzed. The evolution of the concentration according to treatment time was determined for homogeneous EF at  $8.3 \text{ mA cm}^{-2}$ . An initial increase of the concentration was observed until  $t = 6 \text{ h}$  ( $[\Sigma \text{ carboxylic acids}] = 55 \text{ mgC L}^{-1}$ ) because of the degradation of aromatic pollutants. Then, the concentration decreased ( $[\Sigma \text{ carboxylic acids}] = 34 \text{ mgC L}^{-1}$  at  $t = 8 \text{ h}$ ). In fact, the lower concentration of organic compounds after 6 h of treatment resulted in lower formation rate of carboxylic acids compared to the degradation rate. Interestingly, [Fig. 6A](#) shows a linear correlation ( $R^2 = 0.92$ ) between DOC removal (%) and proportion of carboxylic acids among the residual DOC. This correlation took into consideration all analyzes performed for the different configurations tested. The higher the DOC removal achieved, the higher was the proportion of carboxylic acids among the residual DOC. This result is consistent with the lower reaction rate constant of short-chain carboxylic acids with  $\bullet\text{OH}$  ( $10^7 - 10^8 \text{ M}^{-1} \text{ s}^{-1}$ ) compared to aromatic compounds ( $10^9 - 10^{10} \text{ M}^{-1} \text{ s}^{-1}$ ) from which they are formed ([Oturán et al., 2008](#)). The evolution of the proportion of each single carboxylic acid was also studied ([Fig. 6B](#)). It was noticed that the proportion of acetic acid among total carboxylic acid concentration was continuously increased over time during homogeneous EF at  $8.3 \text{ mA cm}^{-2}$ . This phenomenon is also consistent with the lower reaction rate constant of acetic acid with  $\bullet\text{OH}$  ( $1.6 \times 10^7 \text{ M}^{-1} \text{ s}^{-1}$ ) compared to other carboxylic acids ([Oturán et al., 2008](#)). Similar trend was observed after 8 h of electrolysis using heterogeneous EF at  $8.3 \text{ mA cm}^{-2}$  or  $4.2 \text{ mA cm}^{-2}$  and homogeneous EF at  $4.2 \text{ mA cm}^{-2}$ , i.e. the higher the DOC removal rate ([Fig. 1](#)), the higher the proportion of acetic acid. Heterogeneous EF/AO using  $\text{Ti}_4\text{O}_7$  was the only experiment exhibiting a different trend, thus indicating that  $\text{Ti}_4\text{O}_7$  might modify mineralization mechanisms, compared to Pt anode. Higher proportion of N-containing oxamic acid and lower proportion of acetic acid were observed with  $\text{Ti}_4\text{O}_7$  anode, which might be attributed to the better electro-catalytic ability of  $\text{Ti}_4\text{O}_7$  anode for the degradation of organic nitrogen and acetic acid, compared to Pt anode. As regards to oxamic acid, these results were consistent with 3DEEM. In fact,  $\text{Ti}_4\text{O}_7$  anode further degraded proteins from biopolymers (zone II'), which usually contain high concentration of N (ratio C/N around 3) ([Jacquin et al., 2017](#)). Overall, the increase of the proportion of carboxylic acids over time confirms the suitability of the combination of EAOPs with a biological treatment ([Fig. 3](#)), because of the well-known high biodegradability of such compounds.

### 3.7. Evolution of inorganic species

Mineralization of  $\text{Cl}^-$  and N-containing organic compounds was accompanied by the formation of inorganic ions. The main inorganic species of interest ( $\text{NO}_3^-$ ,  $\text{NH}_4^+$ ,  $\text{ClO}_3^-$  and  $\text{ClO}_4^-$ ) were analyzed by ion chromatography. Results are presented in [Fig. 7](#). In all experiments, a stronger increase of the concentration of  $\text{NH}_4^+$  was observed compared to  $\text{NO}_3^-$  ([Fig. 7A](#) and [B](#)). These results can be explained by (i) the direct release of  $\text{NH}_4^+$  from mineralization of organic nitrogen and (ii) the release of  $\text{NO}_3^-$  followed by reduction of  $\text{NO}_3^-$  into  $\text{NH}_4^+$  at the cathode. Actually, the latter reaction is often observed during EF and AO, while oxidation of  $\text{NH}_4^+$  at the anode is hindered by the positive charge of this ion ([Martin de Vidales et al., 2016](#); [Mousset et al., 2018](#)). The amount of  $\text{NH}_4^+$  in the solution increased with treatment time and current density because of the higher mineralization rate of organic nitrogen ([Fig. 7B](#)). Higher concentration of  $\text{NH}_4^+$  was also obtained using  $\text{Ti}_4\text{O}_7$  anode

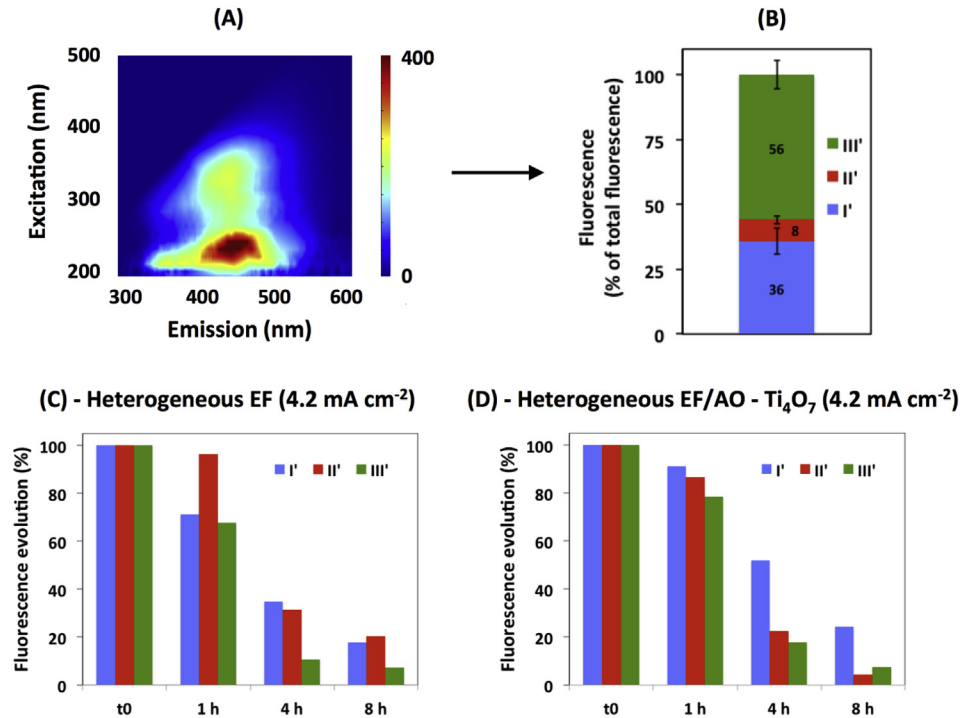


Fig. 5. Fluorescence evolution of the NF concentrate effluent treated by EAOPs, as a function of time treatment. Zone I': colloidal proteins; zone II': Soluble Microbial by-Product (SMP)-like fluorophores; zone III': Humic and Fulvic acids (HA + FA)-like fluorophores.

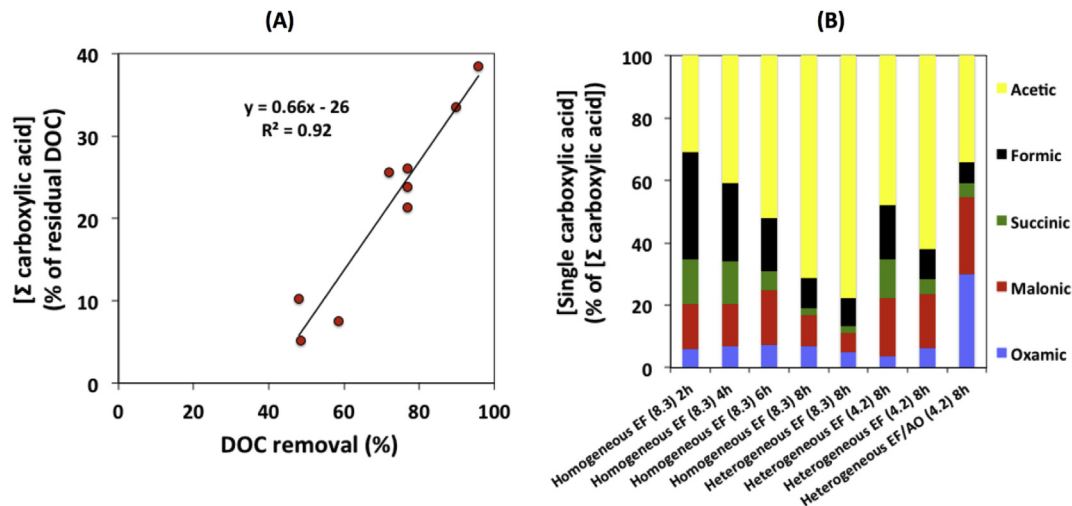
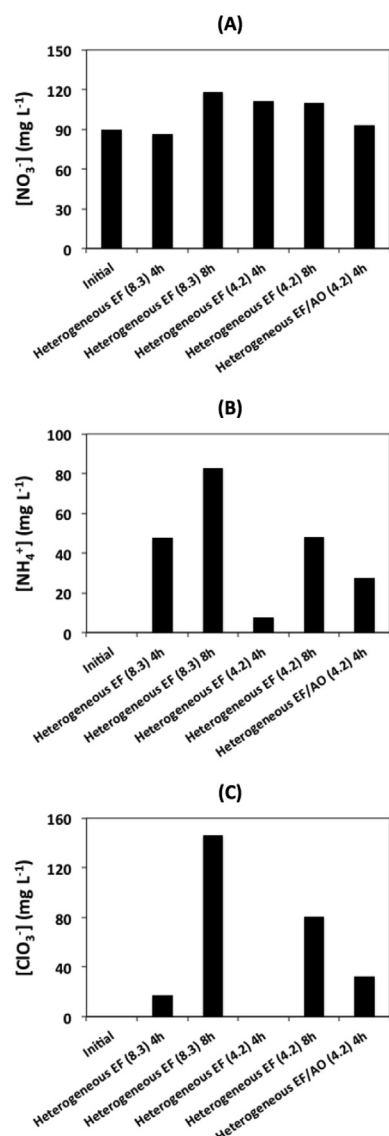


Fig. 6. – Generation of short-chain carboxylic acids during EAOPs: (A) correlation between DOC removal (%) and proportion of carboxylic acids among the residual DOC; (B) evolution of the proportion of each single carboxylic acid among the total carboxylic acid concentration as a function of configurations and operating conditions (current density in bracket,  $\text{mA cm}^{-2}$ ).

(heterogeneous EF/AO), compared to Pt anode (heterogeneous EF). This phenomenon is consistent with the results obtained from 3DEEM and with the higher concentration of oxamic acid previously reported, and supports the higher electro-catalytic activity of  $\text{Ti}_4\text{O}_7$  for the degradation of organic nitrogen. In the context of a treatment strategy including a recirculation of the effluent back to the MBR, the release of  $\text{NH}_4^+$  during EAOPs would require further biological nitrification in the MBR.

Oxidation of  $\text{Cl}^-$  resulted in a strong increase of  $\text{ClO}_3^-$  concentration (Fig. 7C). The reaction mechanisms usually go through  $\text{Cl}^-$  oxidation into  $\text{Cl}_2$ , followed by hydrolysis of  $\text{Cl}_2$  into hypochlorous

acid HOCl. Further oxidation of HOCl lead to the formation of  $\text{ClO}_2^-$  (which was not detected because of the fast oxidation kinetic) and subsequently  $\text{ClO}_3^-$ . No formation of  $\text{ClO}_4^-$  was detected in any experiment because higher current density ( $>30 \text{ mA cm}^{-2}$ ) is required to form this compound (Mousset et al., 2018). Besides, it was also observed that the formation of  $\text{ClO}_3^-$  mainly occurred between 4 and 8 h of treatment, most probably because of the preferential reaction of HOCl with organic species and  $\text{NH}_4^+$  (break-point chlorination) between 4 and 8 h of treatment (Martin de Vidales et al., 2016; Mousset et al., 2018). These results confirm the suitability to stop the treatment after 4 h of treatment in order



**Fig. 7.** Concentration evolution of main inorganic species of interest during EAOPs as a function of configurations and operating conditions (current density in bracket, mA cm<sup>-2</sup>): (A) ClO<sub>3</sub><sup>-</sup>, (B) NO<sub>3</sub><sup>-</sup> and (C) NH<sub>4</sub><sup>+</sup>. ClO<sub>4</sub><sup>-</sup> was not detected.

to avoid the accumulation of ClO<sub>3</sub><sup>-</sup> and NH<sub>4</sub><sup>+</sup>. While ClO<sub>3</sub><sup>-</sup> can be toxic for the biomass in the MBR, the formation of NH<sub>3</sub> at basic pH is also highly toxic for the autotrophic biomass (Jacquin et al., 2018).

#### 4. Conclusion

NF concentrate of landfill leachate pre-treated in a MBR contains high concentration of biorefractory organic pollutants that makes very difficult to treat or detoxify by conventional techniques. The investigation of different configurations of EAOPs applied to this complex effluent showed that heterogeneous EF/AO using Ti<sub>4</sub>O<sub>7</sub> anode and Fe<sup>II</sup>/Fe<sup>III</sup>-LDH modified CF cathode is the most efficient process for mineralization of organic pollutants. Without initial pH adjustment and external addition of Fe<sup>2+</sup> in the bulk, 45% removal of DOC was achieved at 4.2 mA cm<sup>-2</sup> with limited energy consumption (0.11 kWh g<sup>-1</sup> of DOC removed, i.e. 49.5 kWh m<sup>-3</sup>). Up to 96% removal of DOC was also obtained by using higher current density (8.3 mA cm<sup>-2</sup>) during the heterogeneous EF process. The use of Ti<sub>4</sub>O<sub>7</sub> anode appeared to be a key parameter for improving

the degradation and mineralization of organic nitrogen. From 3DEEM analysis, colloidal proteins were observed to be the most refractory organic compounds. Therefore, improving the retention of such compounds in the MBR could improve the efficiency of the EAOP.

The acute toxicity of the effluent was not removed but strong biodegradability enhancement was observed after 4 h of treatment by heterogeneous EF/AO, thus making possible the recirculation of the residual DOC towards the MBR in order to achieve total COD removal without longer electrochemical treatment time. This result was consistent with the identification and quantification of more biodegradable and less toxic by-products such as carboxylic acids. In fact, a linear correlation was observed between DOC removal rate and proportion of carboxylic acids in the residual DOC. As regards to the fate of inorganic species, the formation of ClO<sub>3</sub><sup>-</sup> could be limited by stopping electro-oxidation at 4 h, but enhanced nitrification would be required in the MBR because of the release of NH<sub>4</sub><sup>+</sup> from mineralization of organic nitrogen. Overall, these results emphasized the interdependence between the MBR process and the EAOP in a combined treatment strategy and demonstrated that the use of EAOPs using suitable electrode materials can be useful for the management of such complex effluent.

#### Acknowledgements

We gratefully acknowledge the National French Agency of Research 'ANR' for funding the project ECOTS/CELECTRON. Authors are also grateful to Saint Gobain Research Provence for supplying Ti<sub>4</sub>O<sub>7</sub> electrodes.

#### Appendix A. Supplementary data

Supplementary data to this article can be found online at <https://doi.org/10.1016/j.watres.2019.07.005>.

#### Declaration of interests

The authors declare that they have no known competing financial interests or personal relationships that could have appeared to influence the work reported in this paper.

#### References

- Amaral, M.C., Moravia, W.G., Lange, L.C., Zico, M.R., Magalhães, N.C., Ricci, B.C., Reis, B.G., 2016. Pilot aerobic membrane bioreactor and nanofiltration for municipal landfill leachate treatment. *Journal of Environmental Science and Health, Part A* 51, 640–649.
- Ammar, S., Oturan, M.A., Labiadh, L., Guersalli, A., Abdelhedi, R., Oturan, N., Brillas, E., 2015. Degradation of tyrosol by a novel electro-Fenton process using pyrite as heterogeneous source of iron catalyst. *Water Res.* 74, 77–87. <https://doi.org/10.1016/j.watres.2015.02.006>.
- Brillas, E., Sirés, I., Oturan, M.A., 2009. Electro-fenton process and related electrochemical technologies based on Fenton's reaction chemistry. *Chem. Rev.* 109, 6570–6631. <https://doi.org/10.1021/cr900136g>.
- Campagna, M., Çakmakçı, M., Büşra Yaman, F., Özkaya, B., 2013. Molecular weight distribution of a full-scale landfill leachate treatment by membrane bioreactor and nanofiltration membrane. *Waste Manag.* 33, 866–870. <https://doi.org/10.1016/j.wasman.2012.12.010>.
- Chen, W., Westerhoff, P., Leenheer, J.A., Booksh, K., 2003. Fluorescence Excitation–Emission matrix regional integration to quantify spectra for dissolved organic matter. *Environ. Sci. Technol.* 37, 5701–5710. <https://doi.org/10.1021/es034354c>.
- Cominellis, C., Kapalka, A., Malato, S., Parsons, S.A., Poullos, I., Mantzavinos, D., 2008. Advanced oxidation processes for water treatment: advances and trends for R&D. *J. Chem. Technol. Biotechnol.* 83, 769–776. <https://doi.org/10.1002/jctb.1873>.
- Cui, Y.-H., Xue, W.-J., Yang, S.-Q., Tu, J.-L., Guo, X.-L., Liu, Z.-Q., 2018. Electrochemical/peroxydisulfate/Fe<sup>3+</sup> treatment of landfill leachate nanofiltration concentrate after ultrafiltration. *Chem. Eng. J.* 353, 208–217. <https://doi.org/10.1016/j.cej.2018.07.101>.
- Ganiyu, S.O., Huong Le, T.X., Bechelany, M., Oturan, N., Papirio, S., Esposito, G., van

- Hullebusch, E., Cretin, M., Oturan, M.A., 2018a. Electrochemical mineralization of sulfamethoxazole over wide pH range using FeII/FeIII LDH modified carbon felt cathode: degradation pathway, toxicity and reusability of the modified cathode. *Chem. Eng. J.* 350, 844–855. <https://doi.org/10.1016/j.cej.2018.04.141>.
- Ganiyu, S.O., Le, T.X.H., Bechelany, M., Esposito, G., Hullebusch, E.D. van, Oturan, M.A., Cretin, M., 2017a. A hierarchical CoFe-layered double hydroxide modified carbon-felt cathode for heterogeneous electro-Fenton process. *J. Mater. Chem.* 5, 3655–3666. <https://doi.org/10.1039/C6TA09100H>.
- Ganiyu, S.O., Oturan, N., Raffy, S., Cretin, M., Esmilaire, R., van Hullebusch, E., Esposito, G., Oturan, M.A., 2016. Sub-stoichiometric titanium oxide (Ti4O7) as a suitable ceramic anode for electrooxidation of organic pollutants: a case study of kinetics, mineralization and toxicity assessment of amoxicillin. *Water Res.* 106, 171–182. <https://doi.org/10.1016/j.watres.2016.09.056>.
- Ganiyu, S.O., Oturan, N., Raffy, S., Esposito, G., van Hullebusch, E.D., Cretin, M., Oturan, M.A., 2017b. Use of sub-stoichiometric titanium oxide as a ceramic electrode in anodic oxidation and electro-fenton degradation of the beta-blocker propranolol: degradation kinetics and mineralization pathway. *Electrochim. Acta* 242, 344–354. <https://doi.org/10.1016/j.electacta.2017.05.047>.
- Ganiyu, S.O., Zhou, M., Martínez-Huitle, C.A., 2018b. Heterogeneous electro-Fenton and photoelectro-Fenton processes: a critical review of fundamental principles and application for water/wastewater treatment. *Appl. Catal. B Environ.* 235, 103–129. <https://doi.org/10.1016/j.apcatb.2018.04.044>.
- Ganzenko, O., Huguenot, D., van Hullebusch, E.D., Esposito, G., Oturan, M.A., 2014. Electrochemical advanced oxidation and biological processes for wastewater treatment: a review of the combined approaches. *Environ. Sci. Pollut. Control Ser.* 21, 8493–8524. <https://doi.org/10.1007/s11356-014-2770-6>.
- Ganzenko, O., Trelu, C., Papirio, S., Oturan, N., Huguenot, D., van Hullebusch, E.D., Esposito, G., Oturan, M.A., 2018. Bioelectro-Fenton: evaluation of a combined biological—advanced oxidation treatment for pharmaceutical wastewater. *Environ. Sci. Pollut. Control Ser.* 25, 20283–20292. <https://doi.org/10.1007/s11356-017-8450-6>.
- García-Rodríguez, O., Bañuelos, J.A., El-Ghenymy, A., Godínez, L.A., Brillas, E., Rodríguez-Valadez, F.J., 2016. Use of a carbon felt–iron oxide air-diffusion cathode for the mineralization of Malachite Green dye by heterogeneous electro-Fenton and UVA photoelectro-Fenton processes. *J. Electroanal. Chem.* 767, 40–48. <https://doi.org/10.1016/j.jelechem.2016.01.035>.
- Guo, L., Jing, Y., Chaplin, B.P., 2016. Development and characterization of ultrafiltration TiO<sub>2</sub> magnéli phase reactive electrochemical membranes. *Environ. Sci. Technol.* 50, 1428–1436. <https://doi.org/10.1021/acs.est.5b04366>.
- Hu, Y., Lu, Y., Liu, G., Luo, H., Zhang, R., Cai, X., 2018. Effect of the structure of stacked electro-Fenton reactor on treating nanofiltration concentrate of landfill leachate. *Chemosphere* 202, 191–197. <https://doi.org/10.1016/j.chemosphere.2018.03.103>.
- Iglesias, O., Fernández de Dios, M.A., Pazos, M., Sanromán, M.A., 2013. Using iron-loaded sepiolite obtained by adsorption as a catalyst in the electro-Fenton oxidation of Reactive Black 5. *Environ. Sci. Pollut. Control Ser.* 20, 5983–5993. <https://doi.org/10.1007/s11356-013-1610-4>.
- Jacquin, C., Lesage, G., Traber, J., Pronk, W., Heran, M., 2017. Three-dimensional excitation and emission matrix fluorescence (3DEEM) for quick and pseudo-quantitative determination of protein- and humic-like substances in full-scale membrane bioreactor (MBR). *Water Res.* 118, 82–92. <https://doi.org/10.1016/j.watres.2017.04.009>.
- Jacquin, C., Monnot, M., Hamza, R., Kouadio, Y., Zaviska, F., Merle, T., Lesage, G., Héran, M., 2018. Link between dissolved organic matter transformation and process performance in a membrane bioreactor for urinary nitrogen stabilization. *Environ. Sci.: Water Research & Technology* 4, 806–819. <https://doi.org/10.1039/C8EW00029H>.
- Kjeldsen, P., Barlaz, M.A., Rooker, A.P., Baun, A., Ledin, A., Christensen, T.H., 2002. Present and long-term composition of msw landfill leachate: a review. *Crit. Rev. Environ. Sci. Technol.* 32, 297–336. <https://doi.org/10.1080/10643380290813462>.
- Li, X., Zhu, W., Wu, Y., Wang, C., Zheng, J., Xu, K., Li, J., 2015. Recovery of potassium from landfill leachate concentrates using a combination of cation-exchange membrane electrolysis and magnesium potassium phosphate crystallization. *Separ. Purif. Technol.* 144, 1–7. <https://doi.org/10.1016/j.seppur.2015.01.035>.
- Ma, L., Zhou, M., Ren, G., Yang, W., Liang, L., 2016. A highly energy-efficient flow-through electro-Fenton process for organic pollutants degradation. *Electrochim. Acta* 200, 222–230. <https://doi.org/10.1016/j.electacta.2016.03.181>.
- Mahindrakar, K.V., Rathod, V.K., 2018. Utilization of banana peels for removal of strontium (II) from water. *Environmental Technology & Innovation* 11, 371–383. <https://doi.org/10.1016/j.eti.2018.06.015>.
- Martín de Vidales, M.J., Millán, M., Sáez, C., Cañizares, P., Rodrigo, M.A., 2016. What happens to inorganic nitrogen species during conductive diamond electrochemical oxidation of real wastewater? *Electrochem. Commun.* 67, 65–68. <https://doi.org/10.1016/j.elecom.2016.03.014>.
- Martínez-Huitle, C.A., Rodrigo, M.A., Sirés, I., Scialdone, O., 2015. Single and coupled electrochemical processes and reactors for the abatement of organic water pollutants: a critical review. *Chem. Rev.* 115, 13362–13407. <https://doi.org/10.1021/acs.chemrev.5b00361>.
- Mousset, E., Pontvianne, S., Pons, M.-N., 2018. Fate of inorganic nitrogen species under homogeneous Fenton combined with electro-oxidation/reduction treatments in synthetic solutions and reclaimed municipal wastewater. *Chemosphere* 201, 6–12. <https://doi.org/10.1016/j.chemosphere.2018.02.142>.
- Oller, I., Malato, S., Sánchez-Pérez, J.A., 2011. Combination of Advanced Oxidation Processes and biological treatments for wastewater decontamination—a review. *Sci. Total Environ.* 409, 4141–4166. <https://doi.org/10.1016/j.scitotenv.2010.08.061>.
- Olvera-Vargas, H., Cocervera, T., Oturan, N., Buisson, D., Oturan, M.A., 2015. Bioelectro-Fenton: a sustainable integrated process for removal of organic pollutants from water: application to mineralization of metoprolol. *J. Hazard Mater.* 319, 13–23. <https://doi.org/10.1016/j.jhazmat.2015.12.010>.
- Oturan, M.A., Pimentel, M., Oturan, N., Sirés, I., 2008. Reaction sequence for the mineralization of the short-chain carboxylic acids usually formed upon cleavage of aromatics during electrochemical Fenton treatment. *Electrochim. Acta* 54, 173–182. <https://doi.org/10.1016/j.electacta.2008.08.012>.
- Oturan, N., van Hullebusch, E.D., Zhang, H., Mazeas, L., Budzinski, H., Le Menach, K., Oturan, M.A., 2015. Occurrence and removal of organic micropollutants in landfill leachates treated by electrochemical advanced oxidation processes. *Environ. Sci. Technol.* 49, 12187–12196. <https://doi.org/10.1021/acs.est.5b02809>.
- Özcan, A., Sahin, Y., Kopal, A.S., Oturan, M.A., 2008. Prophan mineralization in aqueous medium by anodic oxidation using boron-doped diamond anode: influence of experimental parameters on degradation kinetics and mineralization efficiency. *Water Res.* 42, 2889–2898. <https://doi.org/10.1016/j.watres.2008.02.027>.
- Panizza, M., Cerisola, G., 2009. Direct and mediated anodic oxidation of organic pollutants. *Chem. Rev.* 109, 6541–6569. <https://doi.org/10.1021/cr9001319>.
- Ponthieu, M., Pinel-Raffaitin, P., Le Hecho, I., Mazeas, L., Amouroux, D., Donard, O.F.X., Potin-Gautier, M., 2007. Speciation analysis of arsenic in landfill leachate. *Water Res.* 41, 3177–3185. <https://doi.org/10.1016/j.watres.2007.04.026>.
- Poza-Nogueiras, V., Rosales, E., Pazos, M., Sanromán, M.A., 2018. Current advances and trends in electro-Fenton process using heterogeneous catalysts—a review. *Chemosphere* 201, 399–416. <https://doi.org/10.1016/j.chemosphere.2018.03.002>.
- Radjenovic, J., Sedlak, D.L., 2015. Challenges and opportunities for electrochemical processes as next-generation technologies for the treatment of contaminated water. *Environ. Sci. Technol.* 49, 11292–11302. <https://doi.org/10.1021/acs.est.5b02414>.
- Reuschenbach, P., Pagga, U., Strotmann, U., 2003. A critical comparison of respirometric biodegradation tests based on OECD 301 and related test methods. *Water Res.* 37, 1571–1582. [https://doi.org/10.1016/S0043-1354\(02\)00528-6](https://doi.org/10.1016/S0043-1354(02)00528-6).
- Sirés, I., Brillas, E., Oturan, M.A., Rodrigo, M.A., Panizza, M., 2014. Electrochemical advanced oxidation processes: today and tomorrow. A review. *Environ. Sci. Pollut. Res.* 21, 8336–8367. <https://doi.org/10.1007/s11356-014-2783-1>.
- Trelu, C., Chaplin, B.P., Coetsier, C., Esmilaire, R., Cerneaux, S., Causserand, C., Cretin, M., 2018a. Electro-oxidation of organic pollutants by reactive electrochemical membranes. *Chemosphere* 208, 159–175. <https://doi.org/10.1016/j.chemosphere.2018.05.026>.
- Trelu, C., Coetsier, C., Rouch, J.-C., Esmilaire, R., Rivallin, M., Cretin, M., Causserand, C., 2018b. Mineralization of organic pollutants by anodic oxidation using reactive electrochemical membrane synthesized from carbothermal reduction of TiO<sub>2</sub>. *Water Res.* 131, 310–319. <https://doi.org/10.1016/j.watres.2017.12.070>.
- Trelu, C., Ganzenko, O., Papirio, S., Pechaud, Y., Oturan, N., Huguenot, D., van Hullebusch, E.D., Esposito, G., Oturan, M.A., 2016a. Combination of anodic oxidation and biological treatment for the removal of phenanthrene and Tween 80 from soil washing solution. *Chem. Eng. J.* 306, 588–596. <https://doi.org/10.1016/j.cej.2016.07.108>.
- Trelu, C., Oturan, N., Pechaud, Y., van Hullebusch, E.D., Esposito, G., Oturan, M.A., 2017. Anodic oxidation of surfactants and organic compounds entrapped in micelles – selective degradation mechanisms and soil washing solution reuse. *Water Res.* 118, 1–11. <https://doi.org/10.1016/j.watres.2017.04.013>.
- Trelu, C., Péchaud, Y., Oturan, N., Mousset, E., Huguenot, D., van Hullebusch, E.D., Esposito, G., Oturan, M.A., 2016b. Comparative study on the removal of humic acids from drinking water by anodic oxidation and electro-Fenton processes: mineralization efficiency and modelling. *Appl. Catal. B Environ.* 194, 32–41. <https://doi.org/10.1016/j.apcatb.2016.04.039>.
- Van der Bruggen, B., Koninckx, A., Vandecasteele, C., 2004. Separation of mono-valent and divalent ions from aqueous solution by electrodialysis and nanofiltration. *Water Res.* 38, 1347–1353. <https://doi.org/10.1016/j.watres.2003.11.008>.
- Van der Bruggen, B., Lejon, L., Vandecasteele, C., 2003. Reuse, treatment, and discharge of the concentrate of pressure-driven membrane processes. *Environ. Sci. Technol.* 37, 3733–3738. <https://doi.org/10.1021/es0201754>.
- Wang, Yujing, Zhao, G., Chai, S., Zhao, H., Wang, Yanbin, 2013. Three-dimensional homogeneous ferrite-carbon aerogel: one pot fabrication and enhanced electro-fenton reactivity. *ACS Appl. Mater. Interfaces* 5, 842–852. <https://doi.org/10.1021/am302437a>.
- Westerhoff, P., Prapaipong, P., Shock, E., Hillaireau, A., 2008. Antimony leaching from polyethylene terephthalate (PET) plastic used for bottled drinking water. *Water Res.* 42, 551–556. <https://doi.org/10.1016/j.watres.2007.07.048>.
- Xu, Y., Chen, C., Li, X., Lin, J., Liao, Y., Jin, Z., 2017. Recovery of humic substances from leachate nanofiltration concentrate by a two-stage process of tight ultrafiltration membrane. *J. Clean. Prod.* 161, 84–94. <https://doi.org/10.1016/j.jclepro.2017.05.095>.
- Zhang, G., Wang, S., Yang, F., 2012. Efficient adsorption and combined heterogeneous/homogeneous Fenton oxidation of amaranth using supported nano-FeOOH as cathodic catalysts. *J. Phys. Chem. C* 116, 3623–3634. <https://doi.org/10.1021/jp210167b>.
- Zhang, H., Fei, C., Zhang, D., Tang, F., 2007. Degradation of 4-nitrophenol in aqueous

- medium by electro-Fenton method. *J. Hazard Mater.* 145, 227–232. <https://doi.org/10.1016/j.jhazmat.2006.11.016>.
- Zhang, L., Li, A., Lu, Y., Yan, L., Zhong, S., Deng, C., 2009. Characterization and removal of dissolved organic matter (DOM) from landfill leachate rejected by nanofiltration. *Waste Manag.* 29, 1035–1040. <https://doi.org/10.1016/j.wasman.2008.08.020>.
- Zhang, Q.-Q., Tian, B.-H., Zhang, X., Ghulam, A., Fang, C.-R., He, R., 2013. Investigation on characteristics of leachate and concentrated leachate in three landfill leachate treatment plants. *Waste Manag.* 33, 2277–2286. <https://doi.org/10.1016/j.wasman.2013.07.021>.